6-1-2020

Hartree-Fock-Bogoliubov theory of trapped one-dimensional imbalanced Fermi systems

Daniel E. Sheehy
Louisiana State University

Recommended Citation

Sheehy, D. (2020). Hartree-Fock-Bogoliubov theory of trapped one-dimensional imbalanced Fermi systems. *Physical Review A, 101* (6) https://doi.org/10.1103/PhysRevA.101.063607

Hartree-Fock-Bogoliubov theory of trapped one-dimensional imbalanced Fermi systems

Kelly R. Patton[1,*] and Daniel E. Sheehy[2]

[1] *Department of Physics & Astronomy, Georgia Southern University-Armstrong Campus, Savannah, GA 31419, USA*
[2] *Department of Physics & Astronomy, Louisiana State University, Baton Rouge, Louisiana 70803, USA*

(Dated: March 27, 2020)

Ground state Hartree-Fock-Bogoliubov (HFB) theory is applied to imbalanced spin-1/2 one-dimensional Fermi systems that are spatially confined by either a harmonic or a hard-wall trapping potential. It has been hoped that such systems, which can be realized using ultracold atomic gases, would exhibit the long-sought-after Fulde-Ferrell-Larkin-Ovchinnikov (FFLO) superfluid phase. The HFB formalism generalizes the standard Bogoliubov quasi-particle transformation, by allowing for Cooper pairing to exist between all possible single-particle states, and accounts for the effects of the inhomogeneous trapping potential as well as the mean-field Hartree potential. This provides an unbiased framework to describe inhomgenous densities and pairing correlations in the FFLO state of a confined 1D gas. In a harmonic trap, numerical minimization of the HFB ground state energy yields a spatially oscillating order parameter reminiscent of the FFLO state. However, we find that this state has almost no imprint in the local fermion densities (consistent with experiments that found no evidence of the FFLO phase). In contrast, for a hard-wall geometry, we find a strong signature of the spatial oscillations of the FFLO pairing amplitude reflected in the local *in situ* densities. In the hard wall case, the excess spins are strongly localized near regions where there is a node in the pairing amplitude, creating an unmistakeable crystalline modulation of the density.

I. INTRODUCTION

Irrespective of the temperature, applying a sufficiently strong external magnetic field to a superconductor destroys the superconducting state. For a conventional superconductor, a spin-imbalanced Fermi liquid becomes the energetically favored phase above this critical field strength. Driving this phase transition is the mismatch of the spin-↑ and spin-↓ Fermi energies, which is a consequence of the Zeeman splitting caused by the applied magnetic field. Within Bardeen Cooper Schrieffer (BCS) theory [1], for an s-wave superconductor and weak interactions, once the Zeeman splitting reaches a critical value, on the order of the superconducting gap Δ, the so-called Chandrasekhar-Clogston limit [2, 3], the superconducting state is no longer energetically favorable. Depending on the effective dimensionality and interaction strength, a similar phase transition can occur in neutral fermionic superfluids, which are now commonly realized using ultracold atomic gases. In such systems, the mismatch of Fermi energies is accomplished by selectively populating two pseudo-spin-1/2 hyperfine states of the atoms. Thus, in contrast with an archetypal condensed matter system, the spin imbalance in ultracold atomic gases can be readily fine-tuned across the full parameter range, from zero imbalance, equal numbers of each spin, to fully polarized.

The Fermi liquid phase is not the only possibility for fields greater than the Chandrasekhar-Clogston limit. Indeed, several unconventional superconducting/fluid phases have been theoretically predicted to exist in this regime. One such phase is the Fulde-Ferrell-Larkin-Ovchinnikov (FFLO) state [4, 5], which has attracted considerable attention for many years. Unlike a conventional fermionic superfluid, where the Cooper pairs have zero net momentum, the FFLO state is comprised of pairs having momentum $\boldsymbol{Q}$. In a translationally invariant system and at weak coupling, it can be shown that $\boldsymbol{Q} \approx \boldsymbol{k}_{\rm F}^{\uparrow} - \boldsymbol{k}_{\rm F}^{\downarrow}$, where $\boldsymbol{k}_{\rm F}^{\sigma}$ are the Fermi wave vectors of

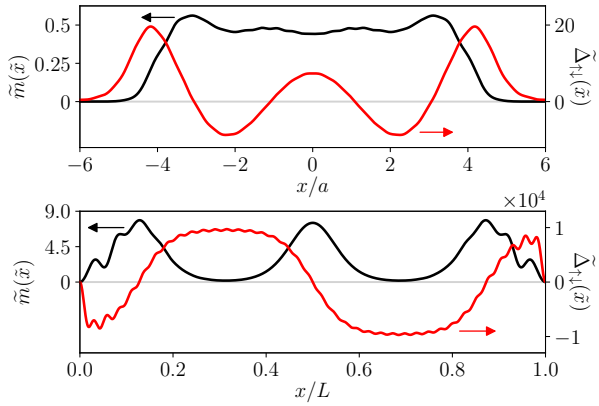

FIG. 1. (Color online) The top and bottom panels each show the local magnetization (black curves) and pairing amplitude (red curves) for a one-dimensional imbalanced Fermi superfluid confined in a parabolic single-particle potential (top panel) and a homogeneous box trap (bottom panel). While each case shows oscillatory pairing correlations reminiscent of an FFLO [4, 5] phase, the signature of such pairing in the local density is much stronger in the case of a box trap. The arrows indicate which y-axis each curve corresponds to. (All parameters are the same as in Figs. 2 and 3.)

*kpatton@georgiasouthern.edu

each spin. This momentum corresponds to a periodic real space order parameter $\Delta(\boldsymbol{r}) = \Delta(\boldsymbol{r}+\boldsymbol{a})$, where the lattice constant $|\boldsymbol{a}| \approx 2\pi/|\boldsymbol{Q}|$. Fulde and Ferrell (FF) proposed a plane wave order parameter $\Delta(\boldsymbol{r}) \propto \mathrm{e}^{i\boldsymbol{Q}\cdot\boldsymbol{r}}$, while Larkin and Ovchinnikov (LO) proposed a standing wave version $\Delta(\boldsymbol{r}) \propto \cos(\boldsymbol{Q}\cdot\boldsymbol{r})$. Above the Chandrasekhar-Clogston limit, both are energetically more favorable than a Fermi liquid, but the LO state is believed to have the lowest energy of the two.

In addition to the ground state spontaneously breaking the $U(1)$ symmetry related to fixed particle number, the FF-state order parameter would also break inversion symmetry, while the LO state would break translational invariance. It is thought that the breaking of these additional symmetries, especially for an LO state, would lead to a clear experimental signature in the local density [6]. Indeed, an LO-type superfluid would possess a modulated density that is commensurate with the oscillations of the local pairing function. Physically, this density modulation results from the unpaired atoms, due to the imbalance, localizing near the nodes of the pairing amplitude. As a result, the simultaneous coexistence of a magnetic lattice order and a superfluid would occur. Unfortunately, despite considerable effort over the past sixty years, little to no conclusive experimental evidence of an FFLO state in either ultracold gases [7–22] or condensed matter systems [23, 24] has been found.

As previously mentioned, the particle number of each pseudo-spin is externally controllable in ultracold atomic systems, as well as the atoms' effective spatial dimensionality and inter-particle interactions. These experimental controls make ultracold atomic gases an almost ideal physical system to realize exotic states of matter. While the regime of stability for the FFLO state of a trapped Fermi gas is predicted to be rather narrow in three dimensions [25–27], the situation improves in lower dimensions. In particular, the FFLO phase has been theoretically predicted to be stable over a wide parameter range in one dimension (1D) [28, 29]. Experiments [22] for a harmonically trapped gas in 1D show that at small population imbalances, the gas is locally magnetized only in a central region of the trap, while the edges of the cloud remain unpolarized. The spatial extent of the polarized central region grows with increasing imbalance until a critical polarization P_c is reached, above which the entire cloud becomes magnetic. Nevertheless, no sign of an underlying FFLO-like order parameter is discernible in the *in situ* densities. However, it is unclear how the anisotropic trapping potential, which is omnipresent in ultracold atomic systems and breaks translational symmetry, effects spatially varying phases, such as FFLO, or their detection.

Further uncertainty arises as predictions from different theoretical methods have varying degrees of agreement with each other and the experiments. For example, exact thermodynamic Bethe ansatz combined with the local density approximation (BA+LDA) appears to be consistent with experimental results [28–32]. The results of BA+LDA predict a magnetized central core that grows with increasing polarization. The critical polarization P_c, above which the entire cloud is magnetized, is also in general agreement with the experimental results. In principle, the Bethe ansatz gives the exact many-body wave function, from which the local density can be obtained. Unfortunately, extracting the local density from the many-body wave function is difficult. Thus, the results of Refs. 28–32 only represent the *average* density (total particle number N per volume V: $n = N/V$) in the thermodynamic limit and not the exact local density $n(x)$. The average density in the inhomogeneous trap is found within the LDA, which amounts to replacing the thermodynamic chemical potential (μ) dependence of the average density, $n(\mu)$, by a spatially vary one, $\mu \to \mu - V(x)$, where $V(x)$ is the trapping potential; $n(\mu - V(x))$. Unsurprisingly, the results show no spatial modulation of the average density that would be indicative of an FFLO-like state. To directly take into account the effects of the trapping potential, the present authors put forth a BCS-like variational wave function in Ref. 33. Reminiscent of the experiment and BA+LDA, this wave function also produced magnetized and unmagnetized regions, but, unlike BA+LDA, it further showed LO-like oscillations in the local pairing amplitude. Nonetheless, no signature of these oscillations was reflected in the local *in situ* densities. In contrast, local mean-field theory [34–37] and various lattice models and methods [38–43] tend to show large oscillations in the pairing amplitude that are clearly (in most cases) correlated with a modulation of the local density or magnetization.

In this article, we take yet another approach to the physics of FFLO phases in trapped fermionic atomic gases with an imposed population imbalance. We apply the configuration based Hartree-Fock-Bogoliubov (HFB) [44–47] theory to these systems. HFB theory is a generalization of Hartree-Fock mean-field theory to systems with Cooper pairing. Unlike standard BCS theory, where the Bogoliubov quasi-particles are a linear combination of a single particle and a single hole, in HFB theory, a quasi-particle is represented by a linear combination of all possible particle and hole states. This is of importance because, in a balanced and translationally invariant system, the only particle-particle interaction terms that are meaningful in the renormalization-group (RG) sense are the ones that give rise to the formation of standard Cooper pairs, i.e., the interaction between plane-wave-time-reserved states [48]. However, since the universality class of an infinite FFLO system is currently unknown, it is not clear what the relevant interactions (in the RG sense) in a trapped and/or imbalanced system are. Hartree-Fock-Bogoliubov theory circumvents this ambiguity by allowing for a broad range of pairing and density correlations.

An additional advantage of the HFB approach is that it takes into account the effect of the nontrivial inhomogeneous Hartree potential. The real space, or coordinate, version of HFB has previously been applied to trapped

and imbalanced systems [34–37]. Here, we apply HFB in the single-particle basis, the so-called configuration formalism. This formalism has been highly developed in the nuclear physics community [44]. The benefit of this approach is that it results in more detailed information about the system. For example, besides the local densities and pairing amplitude, one has access to the occupation probability of each level, the pairing amplitude between all single-particle states, the mode resolved single-particle density matrix, or any other equal-time ground state correlation function. This leads to building a richer and more physically intuitive picture of the FFLO state in trapped systems. Additionally, this method allows for optimal control over the size of the Hilbert space needed for numerical calculations as the strength of particle-particle interactions is increased. This will become especially important in higher-dimensional systems where regularization of the two-body interaction potential is necessary. Applying HFB to ultracold atomic gases in higher dimensions will be part of future work.

In the following sections, we present the application of HFB theory to find the mean-field ground state of polarized spin-1/2 fermions in 1D. We obtained results for two specific systems: Fermions with a harmonic (parabolic) confining trap and fermions with a box-shaped (hard-wall, or "homogeneous") confining potential [49, 50]. In the harmonic case, our HFB method agrees with both experiments and BA+LDA theory for observables like the critical P_c, giving us confidence in this method. Our main findings concern the existence and nature (and potential observability) of any FFLO pairing correlations in the presence of these two types of trapping potential. In general, we find that the ground states of both systems, in the polarized regime, are FFLO-like, showing spatial oscillations in both the local pairing amplitude and the local densities. However, the details show significant differences between the two systems as shown in Fig. 1. For the harmonically trapped system, the amplitudes of the density modulations are relatively small, especially in comparison to the hard-wall case, and would probably be entirely washed out at finite temperature [35] or by other experimental limitations (such as imaging resolution). Another striking difference is that unlike the harmonic trap, there is no central region of magnetization in the hard-wall system. Instead, at all polarizations, the system is only magnetic near the nodes of the pairing amplitude with zero magnetization elsewhere, i.e., the local magnetization has a definitive crystalline order. Thus, our results imply that it may be much easier to experimentally detect the FFLO state in a box-shaped trap.

The rest of this Paper is organized as follows. In Sec. II, we present the general HFB theory for a system of fermions in one spatial dimension subject to a trapping potential $V(x)$. In Sec. III we apply the HFB theory to the two specific systems described above, i.e., the case of harmonically trapped atoms characterized by trap frequency ω_0 (i.e., $V(x) = \frac{1}{2}m\omega_0^2 x^2$) and the case of a homogeneous box trap of size L (i.e., $V(x) = 0$ for $0 < x < L$ and $V(x) = \infty$ elsewhere). In Sec. IV, we elaborate on these results and discuss the prospects of their extension and future work.

II. THEORY

Here, for completeness, we recap the salient aspects of HFB theory, which can be found in the literature [44–47], although, unfortunately, with varying notational conventions. In principle, this can be applied to systems of arbitrary dimensionality, but currently we will only be interested in 1D systems.

We take the second quantized 1D Hamiltonian of a trapped interacting spin-1/2 Fermi system to be ($\hbar = 1$):

$$\hat{H} = \sum_{\sigma} \int_{-\infty}^{\infty} \mathrm{d}x\, \hat{\Psi}_\sigma^\dagger(x) \left[-\frac{\nabla^2}{2m} + V(x) \right] \hat{\Psi}_\sigma(x) \tag{1}$$
$$+ \frac{1}{2} \sum_{\sigma,\sigma'} \int_{-\infty}^{\infty} \mathrm{d}x\mathrm{d}x'\, \hat{\Psi}_\sigma^\dagger(x) \hat{\Psi}_{\sigma'}^\dagger(x') U(x-x') \hat{\Psi}_{\sigma'}(x') \hat{\Psi}_\sigma(x),$$

where $V(x)$ is the external trapping potential, and $U(x-x')$ is the two-body interaction. In the following sections we will restrict ourselves to a harmonic or hard-wall trapping potential and assume an attractive short-range interaction, which is common for ultracold atomic gases, but for now the trapping potential and interaction will remain arbitrary.

Expanding the field operators in terms of mode operators, $\hat{\Psi}_\sigma^{(\dagger)}(x) = \sum_n \psi_n^{(*)}(x) \hat{a}_{n\sigma}^{(\dagger)}$, the Hamiltonian becomes

$$\hat{H} = \sum_{n,\sigma} \epsilon_n \hat{a}_{n\sigma}^\dagger \hat{a}_{n\sigma} + \frac{1}{2} \sum_{\sigma,\sigma'} \sum_{i,j,k,l} U_{i,j,k,l} \hat{a}_{i\sigma}^\dagger \hat{a}_{j\sigma'}^\dagger \hat{a}_{k\sigma'} \hat{a}_{l\sigma}, \tag{2}$$

where

$$\int_{-\infty}^{\infty} \mathrm{d}x\, \psi_n^*(x) \left[-\frac{\nabla^2}{2m} + V(x) \right] \psi_{n'}(x) = \delta_{n,n'} \epsilon_n, \tag{3}$$

and

$$U_{i,j,k,l} = \int_{-\infty}^{\infty} \mathrm{d}x\mathrm{d}x'\, \psi_i^*(x) \psi_j^*(x') U(x-x') \psi_k(x') \psi_l(x). \tag{4}$$

Going forward, it will be convenient to express the terms appearing in Eq. (2) using a composite orbital-spin index; $\alpha = (n, \sigma)$. Then, the matrix elements of the kinetic energy and interaction terms are

$$T_{\alpha,\beta} = \delta_{n_\alpha,n_\beta} \delta_{\sigma_\alpha,\sigma_\beta} \epsilon_{n_\alpha} = \delta_{\alpha,\beta} \epsilon_\alpha, \tag{5}$$

and

$$U_{\alpha,\beta,\delta,\gamma} = \delta_{\sigma_\alpha,\sigma_\gamma} \delta_{\sigma_\beta,\sigma_\delta} U_{i_\alpha,j_\beta,k_\delta,l_\gamma}. \tag{6}$$

The full Hamiltonian is, then,

$$\hat{H} = \sum_{\alpha,\beta} T_{\alpha,\beta}\hat{a}^\dagger_\alpha \hat{a}_\beta + \frac{1}{2}\sum_{\alpha,\beta,\delta,\gamma} U_{\alpha,\beta,\delta,\gamma}\hat{a}^\dagger_\alpha \hat{a}^\dagger_\beta \hat{a}_\delta \hat{a}_\gamma, \quad (7)$$

where $\sum_\alpha = \sum_n \sum_\sigma$ etc. It will be further convenient to anti-symmetrize the interaction term, $U_{\alpha,\beta,\delta,\gamma}$, in the last two indices:

$$U_{\alpha,\beta,[\delta,\gamma]} = \frac{1}{2}\left(U_{\alpha,\beta,\delta,\gamma} - U_{\alpha,\beta,\gamma,\delta}\right) \equiv \frac{1}{2}\overline{U}_{\alpha,\beta,\delta,\gamma}. \quad (8)$$

Using Eq. (4) one can show $\overline{U}_{\alpha,\beta,\delta,\gamma}$ has the following symmetry relations:

$$\overline{U}_{\alpha,\beta,\delta,\gamma} = -\overline{U}_{\alpha,\beta,\gamma,\delta} = -\overline{U}_{\beta,\alpha,\delta,\gamma} = \overline{U}_{\beta,\alpha,\gamma,\delta} = \overline{U}^*_{\delta,\gamma,\alpha,\beta} \quad (9)$$

This finally gives [60]

$$\hat{H} = \sum_{\alpha,\beta} T_{\alpha,\beta}\hat{a}^\dagger_\alpha \hat{a}_\beta + \frac{1}{4}\sum_{\alpha,\beta,\delta,\gamma} \overline{U}_{\alpha,\beta,\delta,\gamma}\hat{a}^\dagger_\alpha \hat{a}^\dagger_\beta \hat{a}_\delta \hat{a}_\gamma. \quad (10)$$

The basic idea of HFB theory is to generalize the well-known Bogoliubov-Valatin transformation [51, 52] to allow for the most general transformation to quasi-particle operators, $\hat{\gamma}_\alpha$ and $\hat{\gamma}^\dagger_\alpha$, in terms of the single-particle states. To do this we define:

$$\hat{\gamma}^\dagger_\alpha = \sum_{\alpha'}\left[\left(\boldsymbol{V}^{\mathrm{T}}\right)_{\alpha,\alpha'}\hat{a}_{\alpha'} + \left(\boldsymbol{U}^{\mathrm{T}}\right)_{\alpha,\alpha'}\hat{a}^\dagger_{\alpha'}\right], \quad (11a)$$

$$\hat{\gamma}_\alpha = \sum_{\alpha'}\left[\left(\boldsymbol{V}^{\dagger}\right)_{\alpha,\alpha'}\hat{a}^\dagger_{\alpha'} + \left(\boldsymbol{U}^{\dagger}\right)_{\alpha,\alpha'}\hat{a}_{\alpha'}\right], \quad (11b)$$

where $\boldsymbol{V}$ and $\boldsymbol{U}$ are matrices whose elements are the variational parameters that will used to minimize the mean-field ground state energy. The inverse transformation from quasi-particle back to single-particle operators can be most easily found by first defining the column vector

$$\begin{pmatrix}\hat{\boldsymbol{a}}\\ \hat{\boldsymbol{a}}^\dagger\end{pmatrix} = \begin{pmatrix}\hat{a}_{n_1\uparrow}\\ \hat{a}_{n_2\uparrow}\\ \vdots\\ \hat{a}_{n_1\downarrow}\\ \hat{a}_{n_2\downarrow}\\ \vdots\\ \hat{a}^\dagger_{n_1\uparrow}\\ \vdots\\ \hat{a}^\dagger_{n_1\downarrow}\\ \vdots\end{pmatrix} \quad (12)$$

and similarly for $\begin{pmatrix}\hat{\boldsymbol{\gamma}}\\ \hat{\boldsymbol{\gamma}}^\dagger\end{pmatrix}$. Then the *unitary* transformation, Eq. (11), between the two can then be written in block matrix form as

$$\begin{pmatrix}\hat{\boldsymbol{\gamma}}\\ \hat{\boldsymbol{\gamma}}^\dagger\end{pmatrix} = \begin{pmatrix}\boldsymbol{U}^\dagger & \boldsymbol{V}^\dagger\\ \boldsymbol{V}^{\mathrm{T}} & \boldsymbol{U}^{\mathrm{T}}\end{pmatrix}\begin{pmatrix}\hat{\boldsymbol{a}}\\ \hat{\boldsymbol{a}}^\dagger\end{pmatrix} \equiv \boldsymbol{\mathcal{U}}\begin{pmatrix}\hat{\boldsymbol{a}}\\ \hat{\boldsymbol{a}}^\dagger\end{pmatrix}. \quad (13)$$

By unitarity ($\boldsymbol{\mathcal{U}}^\dagger = \boldsymbol{\mathcal{U}}^{-1}$) of the transformation we require

$$\boldsymbol{\mathcal{U}}^\dagger\boldsymbol{\mathcal{U}} = \boldsymbol{\mathcal{U}}\boldsymbol{\mathcal{U}}^\dagger = \mathbb{1}, \quad (14)$$

where

$$\boldsymbol{\mathcal{U}}^\dagger = \begin{pmatrix}\boldsymbol{U} & \boldsymbol{V}^*\\ \boldsymbol{V} & \boldsymbol{U}^*\end{pmatrix}. \quad (15)$$

Thus from Eqs. (14) and (15) this implies we must have

$$\begin{aligned}\boldsymbol{U}^\dagger\boldsymbol{U} + \boldsymbol{V}^\dagger\boldsymbol{V} &= \mathbb{1}, \qquad & \boldsymbol{U}\boldsymbol{U}^\dagger + \boldsymbol{V}^*\boldsymbol{V}^{\mathrm{T}} &= \mathbb{1},\\ \boldsymbol{U}^{\mathrm{T}}\boldsymbol{V} + \boldsymbol{V}^{\mathrm{T}}\boldsymbol{U} &= \mathbb{0}, & \boldsymbol{U}\boldsymbol{V}^\dagger + \boldsymbol{V}^*\boldsymbol{U}^{\mathrm{T}} &= \mathbb{0}.\end{aligned} \quad (16)$$

Furthermore, from Eq. (13) the inverse transformation is given as

$$\begin{pmatrix}\hat{\boldsymbol{a}}\\ \hat{\boldsymbol{a}}^\dagger\end{pmatrix} = \boldsymbol{\mathcal{U}}^{-1}\begin{pmatrix}\hat{\boldsymbol{\gamma}}\\ \hat{\boldsymbol{\gamma}}^\dagger\end{pmatrix} = \boldsymbol{\mathcal{U}}^\dagger\begin{pmatrix}\hat{\boldsymbol{\gamma}}\\ \hat{\boldsymbol{\gamma}}^\dagger\end{pmatrix}, \quad (17)$$

or explicitly by

$$\hat{a}_\alpha = \sum_{\alpha'}\left(U_{\alpha,\alpha'}\hat{\gamma}_{\alpha'} + V^*_{\alpha,\alpha'}\hat{\gamma}^\dagger_{\alpha'}\right), \quad (18a)$$

$$\hat{a}^\dagger_\alpha = \sum_{\alpha'}\left(V_{\alpha,\alpha'}\hat{\gamma}_{\alpha'} + U^*_{\alpha,\alpha'}\hat{\gamma}^\dagger_{\alpha'}\right). \quad (18b)$$

Next we assume a (unnormalized) mean-field ground state of the form $|\Phi\rangle = \prod_\alpha \hat{\gamma}_\alpha|\mathrm{vac}\rangle$. The mean-field ground state acts as a quasi-particle vacuum and satisfies $\hat{\gamma}_\alpha|\Phi\rangle = 0$ for all α. This implies $\langle\Phi|\hat{\gamma}^\dagger_\alpha\hat{\gamma}_{\alpha'}|\Phi\rangle = 0$. We further require that there be no residual pairing between quasi-particles in the ground state, i.e.,

$$\langle\Phi|\hat{\gamma}_\alpha\hat{\gamma}_{\alpha'}|\Phi\rangle = \langle\Phi|\hat{\gamma}^\dagger_\alpha\hat{\gamma}^\dagger_{\alpha'}|\Phi\rangle = 0. \quad (19)$$

Thus the one-body density matrix in the single-particle basis is given by

$$\begin{aligned}\rho_{\alpha,\alpha'} &\equiv \frac{\langle\Phi|\hat{a}^\dagger_\alpha\hat{a}_{\alpha'}|\Phi\rangle}{\langle\Phi|\Phi\rangle} = \sum_\beta V_{\alpha,\beta}V^*_{\alpha',\beta},\\ &= \left(\boldsymbol{V}\boldsymbol{V}^\dagger\right)_{\alpha,\alpha'}\end{aligned} \quad (20)$$

and similarly for the anomalous one-body density matrix

$$\begin{aligned}\kappa_{\alpha,\alpha'} &\equiv \frac{\langle\Phi|\hat{a}_\alpha\hat{a}_{\alpha'}|\Phi\rangle}{\langle\Phi|\Phi\rangle} = \sum_\beta U_{\alpha,\beta}V^*_{\alpha',\beta},\\ &= \left(\boldsymbol{U}\boldsymbol{V}^\dagger\right)_{\alpha,\alpha'}.\end{aligned} \quad (21)$$

One can show that these quantities obey the following symmetry conditions

$$\boldsymbol{\rho} = \boldsymbol{\rho}^\dagger \qquad \text{and} \qquad \boldsymbol{\kappa}^* = -\boldsymbol{\kappa}^\dagger. \quad (22)$$

Using Eqs. (18) the full Hamiltonian, Eq. (10), can be expressed in terms of quasi-particle operators as

$$\hat{H} = E_0 + \hat{H}_{1\mathrm{b}} + \hat{H}_{2\mathrm{b}}, \quad (23)$$

where

$$E_0 = \mathrm{Tr}\left(\boldsymbol{T}\boldsymbol{\rho}^* - \frac{1}{2}\boldsymbol{\Gamma}\boldsymbol{\rho}^* + \frac{1}{2}\boldsymbol{\Delta}\boldsymbol{\kappa}^*\right), \tag{24}$$

is the quasi-particle mean-field ground (vacuum) state energy, and $\hat{H}_{1\mathrm{b}}$ and $\hat{H}_{2\mathrm{b}}$ are one- and two-body quasi-particle operator terms. The one- and two-body terms are not of use in the present work and are quite lengthy, and thus, will not be explicitly given here. The inclusion of these terms would be necessary for excited quasi-particle states, for a finite temperature, or the inclusion of quasi-particle interactions, which we do not consider here. They can be found in the literature, for example, see Ref. 53. In Eq. (24) we have also defined the Hartree energy $\Gamma_{\alpha,\delta}$ and pairing matrix $\Delta_{\alpha,\beta}$ as

$$\Gamma_{\alpha,\delta} = \sum_{\beta,\gamma} \overline{U}_{\alpha,\beta,\delta,\gamma}\rho^*_{\gamma,\beta} \tag{25}$$

$$\Delta_{\alpha,\beta} = \frac{1}{2}\sum_{\delta,\gamma} \overline{U}_{\alpha,\beta,\delta,\gamma}\kappa_{\delta,\gamma}. \tag{26}$$

Similarly, the local spin-resolved densities, magnetization, and pairing amplitude are given by

$$n_\sigma(x) = \sum_{n,n'} \psi^*_n(x)\psi_{n'}(x)\rho_{n\sigma,n'\sigma}, \tag{27}$$

$$m(x) = n_\uparrow(x) - n_\downarrow(x), \tag{28}$$

and

$$\Delta_{\sigma,\sigma'}(x) = \sum_{n,n'} \psi_n(x)\psi_{n'}(x)\kappa_{n\sigma,n'\sigma'} \tag{29}$$

respectively.

Finally, we seek to numerically minimize the ground state energy E_0, Eq. (24), as a function of the matrices $\boldsymbol{U}$ and $\boldsymbol{V}$, subject to the unitary constraints Eqs. (16), the symmetry relations of $\boldsymbol{\rho}$ and $\boldsymbol{\kappa}$ given in Eq. (22), and the total particle number constraint

$$N = \mathrm{Tr}\,\boldsymbol{\rho} = \mathrm{Tr}\,\boldsymbol{V}\boldsymbol{V}^\dagger. \tag{30}$$

In an imbalanced gas with different numbers for spin-↑ and spin-↓

$$N_\uparrow = \sum_n \rho_{n\uparrow,n\uparrow} \qquad \text{and} \qquad N_\downarrow = \sum_n \rho_{n\downarrow,n\downarrow}, \tag{31}$$

are the relevant constraints.

Because the ground state energy, Eq. (24), is expressed in terms of $\boldsymbol{\rho}$ and $\boldsymbol{\kappa}$ it is natural to use their matrix elements as the variables of minimization as opposed to the matrix elements of $\boldsymbol{U}$ and $\boldsymbol{V}$, which appear in the unitary constraints, Eqs. (16). Using the definitions of $\boldsymbol{\rho}$ and $\boldsymbol{\kappa}$ given in Eq. (20) and Eq. (21), one can show that the unitary constraints also be expressed as:

$$\boldsymbol{\kappa}^{\mathrm{T}} + \boldsymbol{\kappa} = \mathbb{0}, \tag{32a}$$

$$\boldsymbol{\kappa}\boldsymbol{\rho} - \boldsymbol{\rho}\boldsymbol{\kappa} = \mathbb{0}, \tag{32b}$$

$$\boldsymbol{\rho}^2 - \boldsymbol{\rho} - \boldsymbol{\kappa}^*\boldsymbol{\kappa} = \mathbb{0}. \tag{32c}$$

Along with the condition $\boldsymbol{\rho} = \boldsymbol{\rho}^\dagger$ this completes the minimization constraints.

III. RESULTS

Our next task is to apply the HFB formalism outlined in the previous section to scenarios that are relevant to recent experiments in ultracold atomic gases, namely spatially confined one-dimensional imbalanced spin-1/2 Fermi systems. In Sec. III A, the external trapping potential is chosen to be harmonic and in Sec. III B a hard-wall box is assumed. For both setups we use a short-ranged particle-particle interaction $U(x-x') = \lambda\delta(x-x')$, which is relevant for dilute ultracold atomic gases.

We will further simplify the problem by assuming both $\boldsymbol{\rho}$ and $\boldsymbol{\kappa}$ are real. This choice precludes a complex FF-type pairing amplitude. Our justification for this assumption is that the LO-type state (in which pairing is real) is believed to be energetically more stable [5]; nonetheless, relaxing this simplification will be left for future work. With this assumption, the HFB ground state energy and constraint conditions become,

$$E_0 = \mathrm{Tr}\left(\boldsymbol{T}\boldsymbol{\rho} - \frac{1}{2}\boldsymbol{\Gamma}\boldsymbol{\rho} + \frac{1}{2}\boldsymbol{\Delta}\boldsymbol{\kappa}\right), \tag{33}$$

and

$$N_\uparrow = \sum_n \rho_{n\uparrow,n\uparrow} \qquad \text{and} \qquad N_\downarrow = \sum_n \rho_{n\downarrow,n\downarrow}, \tag{34}$$

along with

$$\boldsymbol{\rho} = \boldsymbol{\rho}^{\mathrm{T}}, \tag{35a}$$

$$\boldsymbol{\kappa} = -\boldsymbol{\kappa}^{\mathrm{T}}, \tag{35b}$$

$$\boldsymbol{\kappa}\boldsymbol{\rho} = \boldsymbol{\rho}\boldsymbol{\kappa}, \tag{35c}$$

$$\boldsymbol{\rho}^2 - \boldsymbol{\rho} = \boldsymbol{\kappa}\boldsymbol{\kappa}. \tag{35d}$$

The solution to a large scale constrained non-linear minimization problem is needed to find the ground state energy. The open-source software IPOPT [54] was used for this purpose. In principle, both $\boldsymbol{\rho}$ and $\boldsymbol{\kappa}$ are infinite-dimensional matrices, but for computational purposes, a finite representation must be used. In a subspace of the full Hilbert space, each matrix has a linear size of $2\mathcal{D}$, where the 2 accounts for the spin and $\mathcal{D}$ is the dimension of the subspace. For both trapping potentials, we used $\mathcal{D} = 40$. This amounts to a minimization problem in approximately 13,000 variables, the total matrix elements of $\boldsymbol{\rho}$ and $\boldsymbol{\kappa}$. With this cutoff, the number of particles, and interaction strength λ used in the calculations, the occupation of the highest state in the restricted Hilbert space remains only at the 1% level, for either trapping potential.

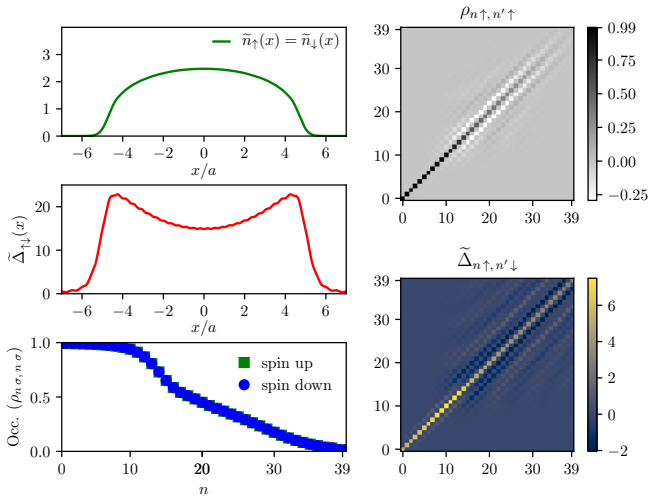

a) $N_\uparrow = N_\downarrow = 20$ ($P = 0$)

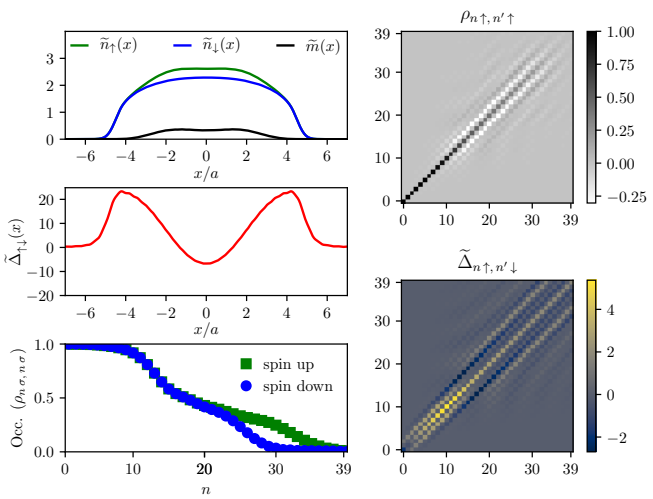

b) $N_\uparrow = 20$ and $N_\downarrow = 18$ ($P \approx 0.05$)

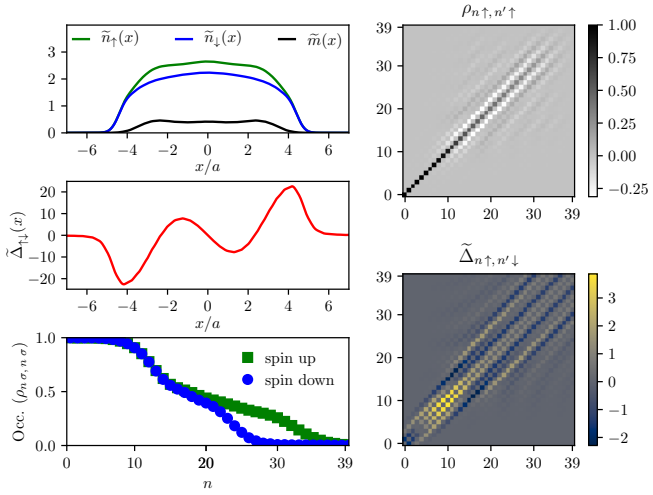

c) $N_\uparrow = 20$ and $N_\downarrow = 17$ ($P \approx 0.08$)

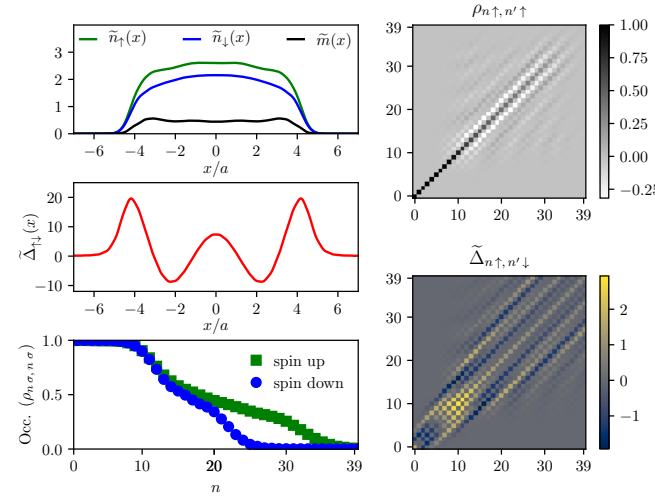

d) $N_\uparrow = 20$ and $N_\downarrow = 16$ ($P \approx 0.11$)

FIG. 2. (Color online) Harmonic trap case: In each panel, Figs. 2a-2d, the dimensionless form of the ground state local spin-resolved densities $\tilde{n}_\sigma(x) = a\, n_\sigma(a\,\tilde{x})$, magnetization $\tilde{m}(x) = \tilde{n}_\uparrow(x) - \tilde{n}_\downarrow(x)$, and pairing amplitude $\tilde{\Delta}_{\sigma,\sigma'}(x) = a\,\omega_0^{-1}\,\Delta_{\sigma,\sigma'}(a\,\tilde{x})$ for a harmonic trapping potential are shown for various spin polarizations $P = (N_\uparrow - N_\downarrow)/(N_\uparrow + N_\downarrow)$, where ω_0 and a are the harmonic trap frequency and oscillator length respectively. In addition, for each polarization the one-body density matrix $\rho_{\alpha,\beta}$, the occupations of the harmonic states $\rho_{\alpha,\alpha}$, and pairing matrix $\tilde{\Delta}_{\alpha,\beta} = \omega_0^{-1}\,\Delta_{\alpha,\beta}$ are also shown. The dimensionless interaction strength for all plots is $\tilde{\lambda} = (\omega_0 a)^{-1}\lambda = -100/\pi^2$.

A. Harmonic Trap

In this section we specialize the general formalism of Sec. II to the case of a harmonically trapped gas with a short-ranged two-body interaction. The external trapping potential of a 1D harmonic oscillator with trapping frequency ω_0 is taken to be

$$V(x) = \frac{1}{2} m\,\omega_0^2 x^2, \tag{36}$$

and single-particle wave functions of $V(x)$ are the well-known harmonic oscillator states

$$\psi_n(x) = \frac{1}{\sqrt{2^n n! a \sqrt{\pi}}} e^{-x^2/(2a^2)} H_n(x/a), \tag{37}$$

where $H_n(x)$ are the Hermite polynomials and $a = (m\omega_0)^{-1/2}$ is the oscillator length. The allowed principal quantum numbers are $n = 0, 1, 2, 3, \ldots$, and the single-particle spectrum is $\epsilon_n = \omega_0(n + 1/2)$. Using the above oscillator states and a delta function interaction, the matrix elements of the two-body interaction term, Eq. (4), are given by

$$U_{n_1,n_2,n_3,n_4} = \lambda \int_{-\infty}^{\infty} \mathrm{d}x\, \psi^*_{n_1}(x)\psi^*_{n_2}(x)\psi_{n_3}(x)\psi_{n_4}(x)$$
$$= \begin{cases} 0 & \text{if } 2M \text{ is odd} \\ \frac{\lambda}{\pi a}(-1)^{M-n_3-n_1}2^{-1/2}(n_1!n_2!n_3!n_4!)^{-1/2}\frac{\Gamma(M-n_2+1/2)\Gamma(M-n_4+1/2)}{\Gamma(M-n_2-n_4+1/2)} & \\ \quad \times {}_3F_2(-n_1,-n_3,-M+n_2+n_4+1/2;-M+n_4+1/2,-M+n_2+1/2;1) & \text{if } 2M \text{ is even,} \end{cases} \tag{38}$$

where $2M = n_1 + n_2 + n_3 + n_4$, $\Gamma(x)$ is the standard gamma function, and ${}_3F_2(a_1, a_2, a_3; b_1, b_2; z)$ is a hypergeometric function. In the evaluation of Eq. (38) one needs to integrate the product of four Hermite polynomials times a Gaussian. This integral can be found in Ref. 55.

The four panels of Fig. 2 depict our results for the evolution of a harmonically trapped 1D Fermi gas for four different values of the total polarization $P = (N_\uparrow - N_\downarrow)/(N_\uparrow + N_\downarrow)$ at fixed interaction strength. Each panel shows the local spin-resolved densities $n_\sigma(x)$ (Eq. (27)), the local magnetization $m(x)$ (Eq. (28)), the local pairing amplitude $\Delta_{\sigma,\sigma'}(x)$ the one-body mode-resolved density matrix $\rho_{\alpha,\beta}$ (Eq. (20)), and the pairing matrix $\Delta_{\alpha,\beta}$ (Eq. (26)).

As we have discussed, our primary interest is how FFLO pairing correlations emerge with increasing P and how they would be reflected in the local densities. We start with the balanced case, $P = 0$, shown in Fig. 2a. We find a local density and pairing amplitude that are spatially inhomogeneous due to the imposed trapping potential, with shapes that are consistent with earlier work based on mean-field theory and Bethe ansatz [59]. Furthermore, the one-body density and pairing matrices are mostly diagonal in index space.

Figures 2b-2d show the evolution of these system properties with increasing P, as homogenous pairing is interrupted by the imposed population imbalance. Consistent with early experiment and theory work [22], we find the imposed population imbalance leads to a magnetized central region reflecting a magnetized core and balanced superfluid edges. With increasing P, the magnetized core increases in size until a critical polarization P_c is reached, beyond which the entire cloud is polarized. For the calculations presented here, we find that P_c lies between 0.11 and 0.14. This is in close agreement with experiments that find a $P_c \sim 0.13$ and in qualitative agreement with BA+LDA, which predicts a $P_c \sim 0.17$ [22].

Figures 2b-2d also show that the local pairing amplitude $\Delta_{\uparrow\downarrow}(x)$ is oscillatory in real space in the imbalanced regime, qualitatively consistent with a LO-like pairing function. A key well-known property of the FFLO state is the prediction that the FFLO wave vector Q is proportional to the imbalance. Here, this is reflected in the fact that the number of nodes in $\Delta_{\uparrow\downarrow}(x)$ increases with increasing P. In fact, for the results presented here the number of nodes is precisely $N_\uparrow - N_\downarrow$, since $\Delta_{\uparrow\downarrow}(x)$ shows 2, 3, and 4 nodes in Figs. 2b-2d, respectively. Thus, for each additional "unpaired" majority spin another node in the pairing function is created.

Thus, our results confirm the expectation of an FFLO phase of harmonically-trapped 1D imbalanced Fermi gases, with nodes in the local pairing amplitude. Our next question is how these nodes are reflected in the principal observable in cold atom experiments, i.e., the local atom densities. Unfortunately, as seen in Figs. 2b-2d, the location of the nodes is only weakly reflected in the local densities and magnetization. Even if these small oscillations in the magnetization could be measured, providing a possible signature of the FFLO phase in experiments, we must recall that our results are for the ground state. Finite temperature effects would most certainly suppress these small oscillations even further, making them likely undetectable [35] via a direct imaging of the density. Extending these results to finite temperature [56] will be left for future work.

The nontrivial off-diagonal values seen in the one-body density matrix $\rho_{\alpha,\beta}$ and the pairing matrix $\Delta_{\alpha,\beta}$ signify scattering from the Hartree potential, and more importantly they indicate the fact that the canonically paired states are not simple pairs of harmonic oscillator states, i.e., $\Delta_{n,n'} \not\propto \langle \hat{a}_{n\uparrow}\hat{a}_{n\downarrow}\rangle\delta_{n,n'}$. But by the Bloch-Messiah-Zumino theorem [57, 58] a transformation exists that can bring both $\rho_{\alpha,\beta}$ and $\kappa_{\alpha,\beta}$ into diagonal and canonical form respectively. Thus the Copper paired states can be represented as a linear combination of many harmonic states. Furthermore, with increasing polarization, the off-diagonal spectral weight increases, with no clearly discernible pattern. The nontrivial occupation probabilities $\rho_{\alpha,\alpha}$ of the oscillator states is also indicative of an unusual pairing solution.

B. Hard-Wall Trap

In this section we turn our attention to the case of a hard-wall or "box" shaped trap in one spatial dimension, characterized by the following single-particle potential for

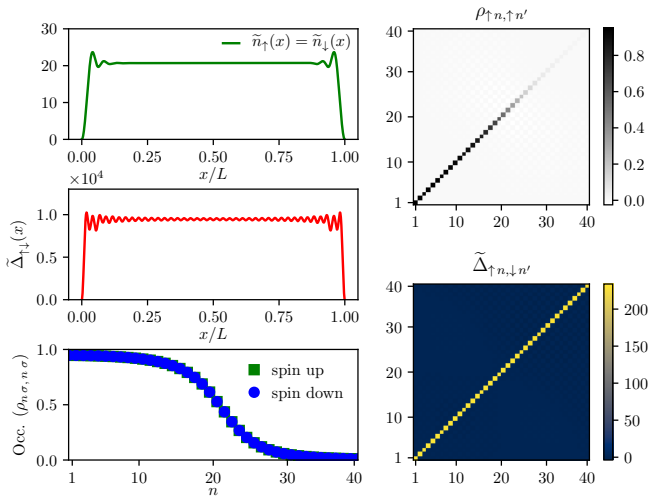

a) $N_\uparrow = N_\downarrow = 20$ ($P = 0$)

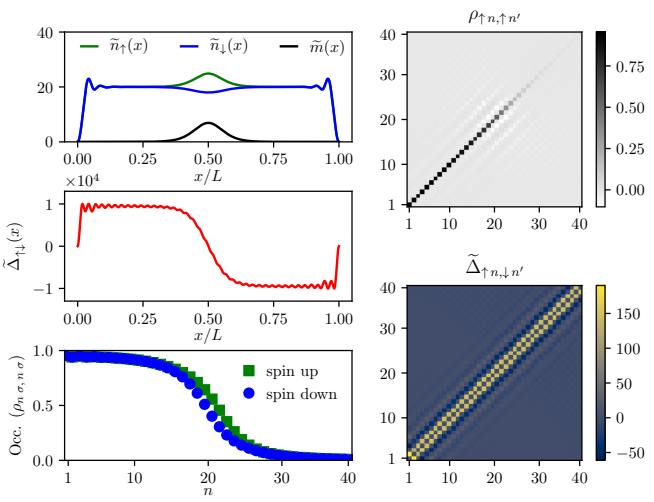

b) $N_\uparrow = 20$ and $N_\downarrow = 19$ ($P \approx 0.025$)

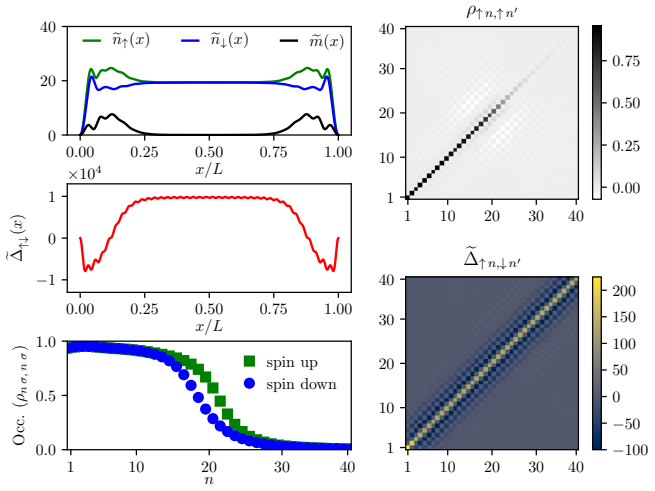

c) $N_\uparrow = 20$ and $N_\downarrow = 18$ ($P \approx 0.05$)

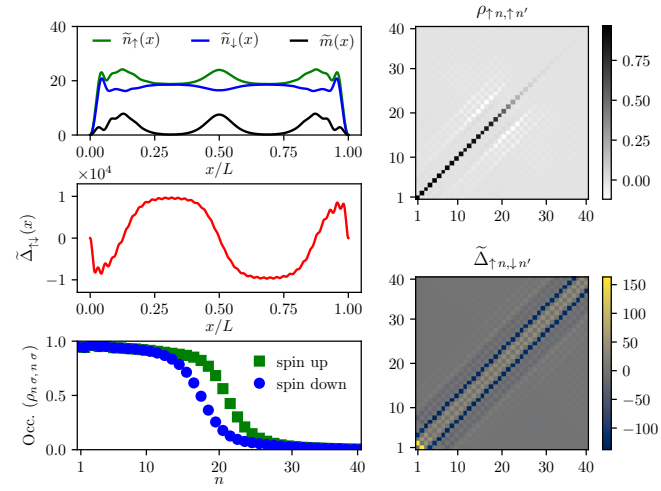

d) $N_\uparrow = 20$ and $N_\downarrow = 17$ ($P \approx 0.08$)

FIG. 3. (Color online) Hard-wall case: In each panel (a-d), the dimensionless form of the ground state local spin-resolved densities $\tilde{n}_\sigma(x) = L\, n_\sigma(L\,\tilde{x})$, magnetization $\tilde{m}(x) = \tilde{n}_\uparrow(x) - \tilde{n}_\downarrow(x)$, and pairing amplitude $\tilde{\Delta}_{\sigma,\sigma'}(x) = L\,\varepsilon^{-1}\,\Delta_{\sigma,\sigma'}(L\,\tilde{x})$ for a hard-wall trapping potential are shown for various spin imbalances $P = (N_\uparrow - N_\downarrow)/(N_\uparrow + N_\downarrow)$, where $\varepsilon = \pi^2/(2mL^2)$, and L is the box length. In addition for each polarization the one-body density matrix $\rho_{\alpha,\beta}$ and pairing matrix $\tilde{\Delta}_{\alpha,\beta} = \varepsilon^{-1}\,\Delta_{\alpha,\beta}$ are also shown. The dimensionless interaction strength for all plots is $\tilde{\lambda} = (\varepsilon L)^{-1}\lambda = -200/\pi^2$.

a 1D infinite square well of width L:

$$V(x) = \begin{cases} 0 & \text{for } 0 \le x \le L \\ \infty & \text{otherwise.} \end{cases} \tag{39}$$

The single-particle spectrum of the well is

$$\epsilon_n = \frac{\pi^2}{2mL^2} n^2 \equiv \varepsilon n^2, \tag{40}$$

where $\varepsilon = \pi^2/(2mL^2)$, which has units of energy ($\hbar = 1$). Numerical results for this system will be shown using ε for an energy scale and L for length. The single-particle states for the potential given by Eq. (39) are the conventional

$$\psi_n(x) = \begin{cases} \sqrt{\frac{2}{L}}\sin(k_n x) & \text{for } 0 \le x \le L \\ 0 & \text{otherwise,} \end{cases} \tag{41}$$

where $k_n = \pi n/L$ with $n = 1, 2, 3, 4, \ldots$. For a short-range interaction, $U(x - x') = \lambda\delta(x - x')$, the matrix elements of the two-body interaction term, Eq. (4), are

then

$$U_{n_1,n_2,n_3,n_4} = \lambda \int_0^L \mathrm{d}x\, \psi^*_{n_1}(x)\psi^*_{n_2}(x)\psi_{n_3}(x)\psi_{n_4}(x),$$
$$= \frac{\lambda}{4L} \sum_{\substack{\varepsilon_1,\varepsilon_2=\pm \\ \varepsilon_3,\varepsilon_4=\pm}} \varepsilon_1\varepsilon_2\varepsilon_3\varepsilon_4\, I(\varepsilon_1 n_1 + \varepsilon_2 n_2 + \varepsilon_3 n_3 + \varepsilon_4 n_4), \tag{42}$$

where $I(n)$ acts like a Kronecker delta function:

$$I(n) = \begin{cases} 1, & \text{if } n = 0 \\ 0, & \text{if } n \neq 0. \end{cases} \tag{43}$$

Our results for the hard-wall case are shown in Fig. 3, where we show the same system properties as in Fig. 2 for four values of the imposed polarization P. Starting with panel (a), $P = 0$, we find essentially homogeneous results for the local density and local pairing amplitude, except for small oscillations near the box edge. Our results for the mode resolved one-body density matrix and pairing matrix of this balanced 1D gas are approximately diagonal, with no unusual structure.

Figures 3b-3d show the fate of this balanced superfluid state under an imposed population imbalance. As in the case of a harmonically trapped gas, such an imbalance leads to a spatially oscillating pair amplitude $\Delta_{\sigma,\sigma'}(x)$, with the number of nodes in the cloud interior being again proportional to $N_\uparrow - N_\downarrow$ and given by $1, 2, 3$ in Figs. 3b, 3c, and 3d respectively. (In this counting we are ignoring the nodes of $\Delta_{\sigma,\sigma'}(x)$ at the edges of the box.)

Although the local pairing in the FFLO state is qualitatively similar to the harmonic case, the reflection of this state in the local atom densities is strikingly different. Indeed, Figs. 3b-3d show relatively narrow peaks in the local density of spin-$\uparrow$ atoms (and corresponding small dips in the local spin-$\downarrow$ density) located spatially near the nodes in $\Delta_{\sigma,\sigma'}(x)$.

Another key difference relative to the harmonic case is that the local magnetization does not exhibit a central polarized region. Instead, the magnetized regions are localized near the nodes of pairing amplitude, with near-zero net magnetization between the nodes. Indeed, this FFLO state can be interpreted in terms of well-formed domain walls in the pairing amplitude, with excess spins-$\uparrow$ congregating near the nodes, providing a robust signature of the FFLO phase of a 1D imbalanced gas in a box trap.

Like the harmonic potential, the mode-resolved one-body density $\rho_{\alpha,\beta}$ and pairing $\Delta_{\alpha,\beta}$ matrices process small but nontrivial off-diagonal spectral weight. Again, this implies that the Cooper pairs of the system are a combination of many single-particle states.

Although the off-diagonal terms of $\rho_{\alpha,\beta}$ are small, these terms are ultimately responsible for the FFLO modulation seen in the density. For example, if the density matrix was diagonal, $\rho_{\alpha,\beta} \propto \delta_{\alpha,\beta}$, then the local density (Eq. (27)), would reduce to $n_\sigma(x) = \sum_n |\psi_n(x)|^2 \rho_{n\sigma,n\sigma}$. Then from Fig. 3 one can see that the occupations probabilities $\rho_{n\sigma,n\sigma}$ are qualitatively similar to what one would expect to see for a non-interacting Fermi gas at some non-zero temperature; thus the density would simply resemble a non-interacting system at a finite temperature and be devoid of any FFLO oscillations.

In this geometry, the off-diagonal terms of the pairing matrix also have a much clearer physical interpretation: the states n and n' that are generally the most strongly paired are those that differ by the particle number imbalance. For example, when $N_\uparrow - N_\downarrow = 3$, shown in Fig. 3d, the states labeled by $n = n' \pm 3$ show the strongest correlations. This implies that under an imbalance, a majority spin in state n tends to most strongly pair with a minority spin in state $n' = n - (N_\uparrow - N_\downarrow)$. This is in agreement with the ansatz put-forth by the present authors in Ref. [33] for a harmonic trap. Here, one imagines that a majority spin at its Femi surface $\epsilon^{\mathrm{F}}_{N_\uparrow}$ will form a pair with a minority spin on the other Fermi surface $\epsilon^{\mathrm{F}}_{N_\downarrow}$.

IV. DISCUSSION AND CONCLUSIONS

The HFB ground state $|\Phi\rangle$, which is also the vacuum state of the generalized Bogoliubov quasi-particles $|\Phi\rangle = \prod_\alpha \hat{\gamma}_\alpha |\mathrm{vac}\rangle$, can also be, by Thouless's theorem [44], expressed as

$$|\Phi\rangle \propto \exp\left(\frac{1}{2}\sum_{\alpha,\beta} Z_{\alpha,\beta}\hat{a}^\dagger_\alpha \hat{a}^\dagger_\beta\right)|\mathrm{vac}\rangle, \tag{44}$$

where $\boldsymbol{Z} = (\boldsymbol{V}\boldsymbol{U}^{-1})^\dagger = (\boldsymbol{\rho}\boldsymbol{\kappa}^{-1})^\dagger$ is an anti-symmetric matrix that gives the probability amplitude of creating a Copper pair comprised of states α and β. Thus in generality state α could form Cooper pairs with many other states, instead of only a single one, as is assumed in the standard BCS wave function, and therefore in the presence of a population imbalance all atoms can still take part in the superfluid state. For the trapped and imbalanced systems considered here, we have found that it is vitally important to account for all possible pairing Hartree-Fock correlations, especially in the harmonic system.

Our analysis shows that while both harmonic and box-shaped traps can host FFLO-like states in the 1D regime, the signature of this state in the harmonic case in the local density is extremely weak and probably unobservable in a real experiment at nonzero temperature. This suggests a competition between the spatial variation of the FFLO state and the slowly-varying potential of the harmonic trap. For the case of a 1D box-shaped trap, however, our results show a striking signature of the FFLO phase in the density profile, indicating that spin-sensitive measurements will be able to discern this exotic state.

Future work will involve generalizing these results to non-zero temperature, which would involve solving a gen-

eralized gap equation for the quasi-particle energy spectrum. This will be essential to determine whether the sharp signatures of the FFLO state in the box trap survive nonzero temperature. Additional future work will extend this formalism to higher dimensions to more generally understand how the spatial profile of the confining potential affects the FFLO phase of an imbalanced Fermi gas and its observability in experimental observables such as the local density.

ACKNOWLEDGMENTS

KRP would like the thank Georgia Southern University for generous startup funding, which contributed to this work.

[1] J. Bardeen, L. N. Cooper, and J. R. Schrieffer, Phys. Rev. **108**, 1175 (1957).
[2] A. M. Clogston, Phys. Rev. Lett. **9**, 266 (1962).
[3] B. S. Chandrasekhar, Appl. Phys. Lett. **1**, 7 (1962).
[4] P. Fulde and R. A. Ferrell, Phys. Rev. **135**, A550 (1964).
[5] A. I. Larkin and Yu. N. Ovchinnikov, Zh. Eksp. Teor. Fiz. **47**, 1136 (1964) [Sov. Phys. JETP **20**, 762 (1965)].
[6] M. W. Zwierlein in *Novel Superfluids Vol. 2*, K. H. Bennemann and J. B. Ketterson (Eds.), Oxford University Press, Oxford, (2014).
[7] M. W. Zwierlein, A. Schirotzek, C.H. Schunck, and W. Ketterle, Science **311**, 492 (2006).
[8] G. B. Partridge, W. Li, R. I. Kamar, Y.-A. Liao, R. G. Hulet, Science **311**, 503 (2006).
[9] Y. Shin, M. W. Zwierlein, C. H. Schunck, A. Schirotzek, W. Ketterle, Phys. Rev. Lett. **97**, 030401 (2006).
[10] G. B. Partridge, W. Li, Y. A. Liao, R. G. Hulet, M. Haque, and H. T. C. Stoof, Phys. Rev. Lett. **97**, 190407 (2006).
[11] N. Navon, S. Nascimbéne, F. Chevy, and C. Salomon, Science **328**, 729 (2010).
[12] B. A. Olsen, M. C. Revelle, J.A. Fry, D. E. Sheehy, and R. G. Hulet, Phys. Rev. A **92**, 053631 (2015).
[13] M. C. Revelle, J. A. Fry, B. A. Olsen, and R. G. Hulet, Phys. Rev. Lett. **117**, 235301 (2016).
[14] A. T. Sommer, L. W. Cheuk, M. J. H. Ku, W. S. Bakr, and M. W. Zwierlein, Phys. Rev. Lett. **108**, 045302 (2012).
[15] Y. Zhang, W. Ong, I. Arakelyan, and J. E. Thomas, Phys. Rev. Lett. **108**, 235302 (2012).
[16] M. G. Ries, A. N. Wenz, G. Zürn, L. Bayha, I. Boettcher, D. Kedar, P.A. Murthy, M. Neidig, T. Lompe, and S. Jochim, Phys. Rev. Lett. **114**, 230401 (2015).
[17] P. A. Murthy, I. Boettcher, L. Bayha, M. Holzmann, D. Kedar, M. Neidig, M. G. Ries, A.N. Wenz, G. Zürn, and S. Jochim, Phys. Rev. Lett. **115**, 010401 (2015).
[18] I. Boettcher, L. Bayha, D. Kedar, P. A. Murthy, M. Neidig, M. G. Ries, A. N. Wenz, G. Zürn, S. Jochim, and T. Enss, Phys. Rev. Lett. **116**, 045303 (2016).
[19] K. Fenech, P. Dyke, T. Peppler, M. G. Lingham, S. Hoinka, H. Hu, and C. J. Vale, Phys. Rev. Lett. **116**, 045302 (2016).
[20] C. Cheng, J. Kangara, I. Arakelyan, and J. E. Thomas, Phys. Rev. A **94**, 031606(R) (2016).
[21] D. Mitra, P. T. Brown, P. Schauß, S.S. Kondov, and W. S. Bakr, Phys. Rev. Lett. **117**, 093601 (2016).
[22] Y. Liao, A. S. Rittner, T. Paprotta, W. Li, G. B. Partidge, R. G. Hulet, S. K. Baur, and E. J. Mueller, Nature **467**, 567 (2010).
[23] H. Mayaffre, S. Krämer, M. Horvatić, C. Berthier, K. Miyagawa, K. Kanoda, and V. F. Mitrović, Nature Phys. **10**, 928 (2014).
[24] J. C. Prestigiacomo, T. J. Liu, and P. W. Adams, Phys. Rev. B **90**, 184519 (2014).
[25] D.E. Sheehy and L. Radzihovsky, Phys. Rev. Lett. **96**, 060401 (2006).
[26] M.M. Parish, F.M. Marchetti, A. Lamacraft, B.D. Simons, Nat. Phys. **3**, 124 (2007).
[27] D.E. Sheehy and L. Radzihovsky, Ann. of Phys. **322**, 1790 (2007).
[28] G. Orso, Phys. Rev. Lett. **98**, 070402 (2007).
[29] H. Hu, X.-J. Liu, and P. D. Drummond, Phys. Rev. Lett. **98**, 070403 (2007).
[30] P. Kakashvili and C. J. Bolech, Phys. Rev. A **79**, 041603 (2009).
[31] E. Zhao, X.-W. Guan, W. V. Liu, M. T. Batchelor, and M. Oshikawa, Phys. Rev. Lett. **103**, 140404 (2009).
[32] X.-W. Guan, M. T. Batchelor, and C. Lee, Rev. Mod. Phys. **85**, 1633 (2013).
[33] K. Patton, D. M. Gautreau, S. Kudla, and D. E. Sheehy, Phys. Rev. A **95**, 063623 (2017).
[34] X.-J. Liu, H. Hu, and P. D. Drummond, Phys. Rev. A **76**, 043605 (2007).
[35] X.-J. Liu, H. Hu, and P. D. Drummond, Phys. Rev. A **78**, 023601 (2008).
[36] H. Lu, L. O. Baksmaty, C. J. Bolech, and H. Pu, Phys. Rev. Lett. **108**, 225302 (2012).
[37] K. Sun and C. J. Bolech, Phys. Rev. A **85**, 051607 (2012).
[38] A. E. Feiguin and F. Heidrich-Meisner, Phys. Rev. B **76**, 220508 (2007).
[39] M. Rizzi, M. Polini, M. A. Cazalilla, M. R. Bakhtiari, M. P. Tosi, and R. Fazio, Phys. Rev. B **77**, 245105 (2008).
[40] M. Tezuka and M. Ueda, Phys. Rev. Lett. **100**, 110403 (2008).
[41] M. R. Bakhtiari, M. J. Leskinen, and P. Törmä, Phys. Rev. Lett. **101**, 120404 (2008).
[42] R. A. Molina, J. Dukelsky, and P. Schmitteckert, Phys. Rev. Lett. **102**, 168901 (2009).
[43] G. G. Batrouni, M. H. Huntley, V. G. Rousseau, and R. T. Scalettar, Phys. Rev. Lett. **100**, 116405 (2008).
[44] R. Ring and P. Schuck, *The Nuclear Many-Body Problem*, Springer-Verlag, Berlin, (1980).
[45] A. L. Goodman in *Advances In Nuclear Physics Vol. 11*, J. W. Negele and E. Vogt (Eds.), Plenum Press, New York-London, (1979).
[46] Y. El Bassem and M. Oulne, Nuclear Physics A **957**, 22 (2017).
[47] J. Dukelsky, G. G. Dussel, and N. M. Sofia, J. Phys. G: Nucl. Phys. **11**, L91 (1985).

[48] J. Polchinski, arXiv:hep-th/9210046
[49] B. Mukherjee, Z. Yan, P. B. Patel, Z. Hadzibabic, T. Yefsah, J. Struck, and M. W. Zwierlein, Phys. Rev. Lett. **118**, 123401 (2017).
[50] K. Hueck, N. Luick, L. Sobirey, J. Siegl, T. Lompe, and H. Moritz, Phys. Rev. Lett. **120**, 060402 (2018).
[51] N. N. Bogoljubov, Il Nuovo Cimento **7** 794 (1958).
[52] J. G. Valatin, Il Nuovo Cimento **7** 843 (1958).
[53] A. Signoracci, T. Duguet, G. Hagen, and G. R. Jansen, Phys. Rev. C **91**, 064320 (2015).
[54] A. Wächer and L. T. Biegler, Math. Program. **16** 25 (2006).
[55] R. D. Lord, Journal of the London Mathematical Society **s1-24**, 101-112 (1949). (Note, there is a typo in Eq. (15). It should read $2^{M-1/2}$ not 2^{M-1}.)
[56] A. L. Goodman, Nuclear Physics A **352**, 30 (1981).
[57] C. Bloch and A. Messiah, Nucl. Phys. **39**, 95 (1962).
[58] B. Zumino, J. Math. Phys. **3**, 1055 (1962).
[59] S. Kudla, D.M. Gautreau, and D.E. Sheehy, Phys. Rev. A **91**, 043612 (2015).
[60] Note that most references dealing with HFB theory do not express the Hamiltonian using Eq. (4), but instead use the two-body matrix element $U^{2\mathrm{b}}_{\alpha,\beta,\delta,\gamma} = \langle\alpha,\beta|U|\delta,\gamma\rangle = \int \mathrm{d}x\mathrm{d}x'\,\psi^*_\alpha(x)\psi^*_\beta(x')U(x-x')\psi_\delta(x)\psi_\gamma(x') = U_{\alpha,\beta,\gamma,\delta}$, which differs from Eq. (4) by the ordering of the last two indices. This difference can lead to minus signs or operator ordering differences from expressions found in the literature when compared to Eq. (7). Nonetheless we stick with using Eq. (4) as it is the most common expression in the ultracold atomic gas community.